

Spin reversal of a rattleback with viscous friction

Hiroshi Takano

Joetsu university of education

943-8512 1 Yamayashiki Joetsu Niigata Japan *

(Dated: December 21, 2011)

Effective equation of motion of a rattleback is obtained from the basic equation of motion with viscous friction depending on slip velocity. This effective equation of motion is used to estimate the number of spin reversals and the rattleback shape that causes the maximum number of spin reversals. These estimates are compared with numerical simulations based on the basic equation of motion.

I. INTRODUCTION

A rattleback, also known as a celt or wobblestone, is a type of mechanical top with the curious property of spin asymmetry. Nowadays, there are different varieties of rattlebacks. Fig. 1 shows a Russian rattleback toy called stubborn tortoise. When the rattleback is spun



FIG. 1. A Russian rattleback toy called stubborn tortoise.

in the clockwise direction which the tortoise has turned to, it continues to spin clockwise until it slows to a stop. However, when the rattleback is spun in the anticlockwise direction, a self induced oscillation occurs, and the spin slows down and eventually its direction is reversed. There is an inertial asymmetry, because the tortoise's center of mass is shifted from the principal axes of the body surface ellipsoid. This inertial asymmetry is responsible for spin reversal.

Many analyses and simulations have attempted to explain the dynamics of rattlebacks during the last century.

The first scientific paper on rattlebacks appeared in 1898 by Walker[1]. Assuming dissipation-free rolling without slipping, he obtained linearized equations of motion for contact point coordinate variables and spin variables. He analyzed the instability of the spin magnitude and direction by studying a characteristic equation and showed the relationship between the direction of spin and

the oscillation. For a realistic case, the spin n is small; therefore, his analysis can explain the behavior of a rattleback.

In 1983, Pascal[2], using the same assumptions as Walker[1], derived effective equations of motion for the slowly varying mode by using the method of averaging and clarified a rattleback's reversal mechanism.

During the same period, Markeev[3] obtained results similar to that of Pascal[2]. He derived two conservation laws and provided a comprehensible explanation of a rattleback's reversal. Their results were extended to second-order averaging by Blackowiak, Rand and Kaplan[4].

Moffatt and Tokieda[5] presented a physically transparent derivation of the effective equations of motion similar to Markeev's derivation.

In 1986, Bondi[6] extended Walker's[1] results to understand how spin evolves for a wide range of geometric and inertial parameters of the body.

For a no-slip dissipation-free case, numerical simulations [7][8][9] showed that infinite spin reversals occur; however, a real rattleback has finite spin reversals because of energy loss by slip friction. Thus, it is important to analyze the dynamics of rattlebacks with slip friction.

Furthermore, Karapetian[10] discussed the stability of rotation of a heavy asymmetric rigid body on a horizontal plane(celtic stone); however, he did not discuss the number of spin reversals. Garcia and Hubbard[9] discussed the limitations of a no-slip case and analyzed the effects of dissipation. They derived augmented equations of motion incorporating lumped models for aerodynamic effects, spinning torque and slipping torque due to Coulomb friction force of slip velocity. In reality, the contact with the horizontal plane is not a point but an area, relative angular motion between the surfaces cause these spinning torque and slipping torque. These equations were solved numerically. Because these equations were too complicated, they presented a simplified model of spin. The spin model derived by considering energy in the spin, oscillation, and dissipation was successful in explaining spin dynamics; however, this model was not derived from equations of motion. Thus, the effect of the slip velocity is not clear. Furthermore, they did not discuss the number of spin reversals and its relationship to the rattleback shape.

The observation of actual behavior of rattlebacks leads to three questions.

* takano@juen.ac.jp

First, for the no-slip case, if the initial spin value n_0 is small, the rattle oscillation becomes large and spin reversal occurs in theory. In contrast, for the slip case, if n_0 is small, the rattle oscillation does not increase, and spin reversal does not occur. In this case, a critical value of the initial spin n_c seems to exist, above which the spin reversal occurs. What is the value of n_c ?

Second, a real rattleback has a finite number of spin reversals because of energy loss by slip friction. When the value of the coefficient of friction is known, how many times does the rattleback reverse and how does the number of spin reversals depend on the coefficient of friction?

Third, it seems that the number of spin reversals depends on the rattleback shape. One rattleback may reverse only once, whereas another may reverse as many as three times. Given that the lower surface of rattleback is defined by an ellipsoid $\frac{x^2}{a^2} + \frac{y^2}{b^2} + \frac{z^2}{c^2} = 1$, where $a > b > c = 1$, if $a \gg b$, the oscillations in the x direction become large and spin reversal occurs rapidly. After one reversal, the oscillations start in the y direction but do not become as large, and spin reversal occurs slowly. In this situation, the number of spin reversals is small. In contrast, if $a = b$, the rattleback is a disk, and spin reversals does not occur. Thus, it seems that a critical ratio of a and b give the maximum number of spin reversals. What is this value?

In this paper, to answer the above questions, I consider the basic equations of motion containing sliding friction and obtain linearized equations of motion containing slip velocity. I derive the effective equations of motion by approximating this velocity. By applying the same averaging method as that used by Pascal[2], differential equations of slowly changing variables are obtained. These differential equations are used to analyze the relationship among the number of spin reversals, the coefficient of friction, and the rattleback shape. The spin behavior obtained from the simulation of the effective equations of motion is compared with that obtained from the simulation of basic equations of motion.

II. BASIC EQUATIONS OF MOTION FOR A RATTLEBACK WITH VISCOUS FRICTION

In this paper, a rattleback is considered to be a uniform ellipsoid of mass m with a smooth lower surface such that $a > b > c$ as follows:

$$\frac{\tilde{x}^2}{a^2} + \frac{\tilde{y}^2}{b^2} + \frac{\tilde{z}^2}{c^2} = 1,$$

where \tilde{x} , \tilde{y} , and \tilde{z} are the body axes of the rattleback as shown in Fig. 2. The distances of the three axes from the center of mass are a , b , and c , respectively. The principal inertia axes are x , y , and z . The z -axis is downward and coincides with \tilde{z} -axis. The axes x - and y -axes are rotated

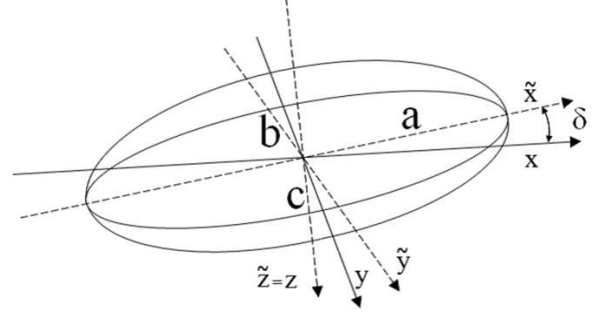


FIG. 2. Body axes \tilde{x} , \tilde{y} , and \tilde{z} with lengths a , b , and c , respectively, principal inertia axes x , y , z and angle δ .

by angle δ such that

$$\begin{pmatrix} \tilde{x} \\ \tilde{y} \end{pmatrix} = \begin{pmatrix} \cos \delta & -\sin \delta \\ \sin \delta & \cos \delta \end{pmatrix} \begin{pmatrix} x \\ y \end{pmatrix},$$

$$\tilde{z} = z.$$

In this paper, it is assumed that δ is small, such as $O(10^{-2})$. The vector at the contact point P , \mathbf{x}_p , has components x , y , and z . \mathbf{u} is the upward unit vector at point P .

When the rattleback rotates, point P is near the point $(0, 0, c)$. When the rattleback is oscillates, the values of x , y are $|x| < a$ and $|y| < b$, respectively, and z can be expanded by a second-order approximation of $\frac{x}{a} < 1$ and $\frac{y}{b} < 1$ as follows:

$$z \simeq c \left(1 - \left\{ \frac{p}{2} \left(\frac{x}{c} \right)^2 + q \frac{xy}{c^2} + \frac{s}{2} \left(\frac{y}{c} \right)^2 \right\} \right),$$

where the parameters p , q , and s are given by

$$p \equiv c^2 \left(\frac{\cos^2 \delta}{a^2} + \frac{\sin^2 \delta}{b^2} \right), \quad (1)$$

$$q \equiv c^2 \cos \delta \sin \delta \left(\frac{1}{b^2} - \frac{1}{a^2} \right), \quad (2)$$

$$s \equiv c^2 \left(\frac{\sin^2 \delta}{a^2} + \frac{\cos^2 \delta}{b^2} \right). \quad (3)$$

At the leading order, the following equations are obtained:

$$\mathbf{x}_p \sim (x, y, 1), \quad (4)$$

$$\mathbf{u} \sim (-px - qy, -qx - sy, -1). \quad (5)$$

Assuming that δ is small, the principal moments of inertia I_{10} , I_{20} , and I_{30} are approximated as follows:

$$I_{10} \simeq mI_1, \quad I_{20} \simeq mI_2, \quad I_{30} \simeq mI_3,$$

where

$$I_1 \equiv \frac{b^2 + c^2}{5}, \quad I_2 \equiv \frac{a^2 + c^2}{5}, \quad I_3 \equiv \frac{a^2 + b^2}{5}.$$

In the following equations, I consider the basic equations of motion for the angular momentum \mathbf{L} and the velocity of the center of mass \mathbf{v}_g . In section VI, numerical simulations of these basic equations of motion are performed. The evolution of angular momentum is governed by Euler's equation:

$$\frac{d}{dt}\mathbf{L} = \mathbf{x}_p \times (R\mathbf{f} + R\mathbf{u}), \quad (6)$$

where $R\mathbf{u}$ is the normal reaction at P , and \mathbf{f} is the slip friction force at P . The dynamics of the center of mass is governed by Newton's equation for the center of mass velocity \mathbf{v}_g :

$$m\frac{d}{dt}\mathbf{v}_g = (R - mg)\mathbf{u} + R\mathbf{f}. \quad (7)$$

The slip velocity, \mathbf{v}_p , is related to velocities $\mathbf{v}_0 \equiv \mathbf{x}_p \times \boldsymbol{\omega}$ and \mathbf{v}_g as follows:

$$\mathbf{v}_p = \mathbf{v}_g - \mathbf{v}_0. \quad (8)$$

Because \mathbf{f} , \mathbf{v}_p , and $\frac{d}{dt}\mathbf{v}_p$ only have components in the horizontal direction, using Eqs. (7) and (8), the normal reaction R is given by

$$R = mg + m\left(\frac{d}{dt}\mathbf{v}_0\right) \cdot \mathbf{u}. \quad (9)$$

The Coulomb law is often used to define sliding friction as follows:

$$\mathbf{f} = -\mu \frac{\mathbf{v}_p}{|\mathbf{v}_p|},$$

where \mathbf{v}_p is the slip velocity and μ is the coefficient of friction. However, this definition of sliding friction is undefined at $\mathbf{v}_p = 0$; therefore, it is difficult to analyze the equations of motion. Thus, in this paper, to understand the dynamics of a rattleback with friction, I shall apply the viscous friction law which states that friction is linearly related to \mathbf{v}_p as follows:

$$\mathbf{f} = -\mu\mathbf{v}_p. \quad (10)$$

The angular momentum \mathbf{L} has components in the principal inertia axes as follows

$$\mathbf{L} = (I_{10}\omega_1, I_{20}\omega_2, I_{30}\omega_3),$$

where ω_i are the components of the angular velocity $\boldsymbol{\omega}$ of the rattleback. $\boldsymbol{\omega}$ is given by the equation $\frac{d}{dt}\mathbf{u} = 0$. In general, because the unit vectors of the principal inertia axes \mathbf{e}_i have time dependence, the time derivative of vector \mathbf{A} is given by

$$\frac{d}{dt}\mathbf{A} = \frac{\partial}{\partial t}\mathbf{A} + (\boldsymbol{\omega} \times \mathbf{A}),$$

where $\frac{\partial}{\partial t}\mathbf{A} \equiv (\frac{d}{dt}A_i)\mathbf{e}_i$. Then

$$\boldsymbol{\omega} = \frac{\partial}{\partial t}\mathbf{u} \times \mathbf{u} + n\mathbf{u}, \quad (11)$$

where $n \equiv \boldsymbol{\omega} \cdot \mathbf{u}$. The dynamical variables of these basic equations of motion are the components of the angular velocity ω_i and the slip velocity v_{pi} .

The equations of motion are obtained by dividing both sides of Eqs. (6) and (7) by g and rescaling of the variables as follows:

$$\begin{aligned} \tilde{t} &= \sqrt{g}t, & \tilde{\mathbf{L}} &= \frac{\mathbf{L}}{\sqrt{g}}, & \tilde{\boldsymbol{\omega}} &= \frac{\boldsymbol{\omega}}{\sqrt{g}}, \\ \tilde{R} &= \frac{R}{g}, & \tilde{\mathbf{v}}_p &= \frac{\mathbf{v}_p}{\sqrt{g}}, & \tilde{\mu} &= \sqrt{g}\mu. \end{aligned}$$

In addition, the length of c is assumed to be unit length, i.e., $c = 1$.

When a rattleback is turned lightly by hand such that the initial value of rotation is $\sim 2\pi$ rad/s, spin reversal occurs. Because $g \sim 980\text{cm/s}^2$, the spin value is $\tilde{n} \sim 0.201$. As spin reversal occurs for this spin value or lower spin values, I assume that $\tilde{n} = \frac{n}{\sqrt{g}} \sim O(10^{-2})$. This assumption is the same as that for the neighborhood of the position of stable equilibrium discussed by Pascal[2]. The value of the order of $\tilde{n} \sim O(10^{-2})$ is used in the next section to approximate the equations of motion.

In the case of limiting μ to infinity, these equations of motion lead to the no-slip case, as shown by the numerical simulation performed in section VI. Therefore, to consider a case in which spin reversal occurs several times, μ is assumed to be not as small as $\tilde{\mu} \sim O(10^2) \sim \frac{1}{\tilde{n}}$.

In the remaining sections, the tilde symbol above the variables is omitted.

III. EFFECTIVE EQUATIONS OF MOTION

In this section, by applying the same linearization method as that of Walker[1] and Pascal[2], the effective equations of motion for a rattleback are obtained. I set $c = 1$ and $n \sim \frac{1}{\mu} \sim O(10^{-2})$, as discussed in the previous section.

The contact point \mathbf{x}_p has components (x, y, z) , which satisfy $\frac{|x|}{a} < 1$, $\frac{|y|}{b} < 1$. The second-order terms can be neglected. Assuming that $\delta \sim O(10^{-2})$, $a \sim O(10)$, and $b \sim O(1)$, as assumed in the numerical simulations, Eqs. (1), (2), and (3) for the parameters p , q , and s are, respectively, approximated as

$$p \simeq \frac{1}{a^2}, \quad q \simeq \frac{\delta}{b^2}, \quad s \simeq \frac{1}{b^2}.$$

These equations imply that the second-order terms of $\sqrt{p}x$, $\sqrt{s}y$, $\sqrt{q}x$, and $\sqrt{q}y$ can be neglected. In addition, the order of the spin value $n \sim O(10^{-2})$ is used, as discussed in the previous section. The second-order terms of n , p , s , and q are also neglected.

For the orders of \dot{x} and \dot{y} , when the time derivative of x is considered, x is multiplied by the oscillation factor. Because a rattleback, unlike a usual top, does not oscillate rapidly, x and \dot{x} are assumed to have the same order. In fact, as Eqs. (45) and (46) will show, the

oscillations are almost $\cos(\nu_{1,2}t)$, and according to Eqs. (34) and (35), $\nu_1^2 \sim \frac{5a^2}{a^2+6}$ and $\nu_2^2 \sim \frac{5b^2}{b^2+6}$, respectively. When $a = 10$ and $b = 3$, as assumed in the simulation in section VI, $\nu_{1,2}$ are $\nu_1^2 \sim 5$ and $\nu_2^2 \sim 3$; thus, it is assumed that $\nu_{1,2} \sim O(1)$. Therefore, the second-order terms of $O(\dot{x}) \sim O(x)$, and $O(\dot{y}) \sim O(y)$, such as $psx\dot{y}$ are neglected.

In this approximation, by using Eqs. (4), (5) and (11), $\boldsymbol{\omega} = (\omega_1, \omega_2, \omega_3)$ has the following components,

$$\boldsymbol{\omega} \simeq (q\dot{x} + s\dot{y}, -p\dot{x} - q\dot{y}, -n), \quad (12)$$

and $\mathbf{v}_0 = \mathbf{x}_p \times \boldsymbol{\omega}$ has components

$$\mathbf{v}_0 \simeq (p\dot{x} + q\dot{y} - n\dot{y}, q\dot{x} + s\dot{y} + n\dot{x}, 0). \quad (13)$$

Because the second term of the time derivative of \mathbf{v}_0 , $\boldsymbol{\omega} \times \mathbf{v}_0$, is second order of n, p, q and s , $\frac{d}{dt}\mathbf{v}_0$ are as follows:

$$\begin{aligned} \frac{d}{dt}\mathbf{v}_0 &\simeq \frac{\partial}{\partial t}\mathbf{v}_0 \\ &\simeq (p\ddot{x} + q\ddot{y} - n\dot{y}, q\ddot{x} + s\ddot{y} + n\dot{x}, 0), \end{aligned} \quad (14)$$

where terms such as $\dot{n}\dot{y}$ are neglected because \dot{n} is the second-order terms, as will be shown in Eq. (26).

In Eq. (9) for R , it is seen from Eqs. (5) and (14) that $(\frac{d}{dt}\mathbf{v}_0) \cdot \mathbf{u}$ is the second-order term; thus, $R \sim m$. Therefore, setting $R = m$ in Eqs. (6) and (7), the following equations are obtained

$$\frac{d}{dt}\mathbf{L} = m(\mathbf{N}_0 + \mathbf{N}_g + \mathbf{N}_p), \quad (15)$$

$$\frac{d}{dt}\mathbf{v}_g = \mathbf{f}, \quad (16)$$

where

$$\mathbf{N}_0 \equiv \mathbf{x}_p \times \frac{d}{dt}\mathbf{v}_0, \quad \mathbf{N}_g \equiv \mathbf{x}_p \times \mathbf{u}, \quad \mathbf{N}_p \equiv \mathbf{x}_p \times \frac{d}{dt}\mathbf{v}_p.$$

These equations contain six dynamical variables: x, y, n , and the components of \mathbf{v}_p . Therefore, it is difficult to analyze of dynamics of these variables.

Using the approximation in Eq. (12) for $\boldsymbol{\omega}$, and neglecting the second-order terms of n, p, q and s , the approximation of $\frac{d}{dt}\mathbf{L}$ has components

$$\frac{d}{dt}\mathbf{L} \simeq (I_1(q\ddot{x} + s\ddot{y}), -I_2(p\ddot{x} + q\ddot{y}), -I_3\dot{n}). \quad (17)$$

At the leading order, \mathbf{N}_0 has components

$$\begin{aligned} N_{01} &\simeq -(q\ddot{x} + s\ddot{y}) - n\dot{x}, \\ N_{02} &\simeq p\ddot{x} + q\ddot{y} - n\dot{y}, \\ N_{03} &\simeq q(x\ddot{x} - y\ddot{y}) + sx\ddot{y} - p\ddot{x}y + n(x\dot{x} + y\dot{y}), \end{aligned} \quad (18)$$

where the approximation $n(1-p)x\dot{x} \sim nx\dot{x}$ is adopted. At the leading order, \mathbf{N}_g has components

$$\mathbf{N}_g \simeq (-y, x, q(y^2 - x^2) + xy(p - s)), \quad (19)$$

where the approximation $qx - (1-s)y \sim -y$ is adopted.

Next, I consider an approximation in which \mathbf{v}_p is expressed by x, y , and n . This approximation is crucial for simplifying these complicated equations of motion. Eqs. (8), (10) and (16) give $\mu\mathbf{v}_p = -\frac{d}{dt}\mathbf{v}_0 - \frac{d}{dt}\mathbf{v}_p$. In addition, the numerical simulation in section VI shows that $\frac{d}{dt}\mathbf{v}_0 \gg \frac{d}{dt}\mathbf{v}_p$; therefore, the following approximation is obtained:

$$\mathbf{v}_p \sim -\frac{1}{\mu} \frac{d}{dt}\mathbf{v}_0. \quad (20)$$

Because the components of \mathbf{v}_0 are given by x, y , and n from Eq. (13), the dynamical variables reduce to x, y , and n as will be shown in Eqs. (29)-(31). It is easily seen from Eqs. (14) and (20) that v_{p3} is second-order term. In addition, the term $\boldsymbol{\omega} \times \mathbf{v}_p$ is neglected in the time derivative of \mathbf{v}_p . Thus, $\frac{d}{dt}\mathbf{v}_p$ has components,

$$\frac{d}{dt}\mathbf{v}_p \sim \frac{\partial}{\partial t}\mathbf{v}_p \sim (\dot{v}_{p1}, \dot{v}_{p2}, 0). \quad (21)$$

Using Eq. (21), \mathbf{N}_p has components

$$\mathbf{N}_p \simeq (-\dot{v}_{p2}, \dot{v}_{p1}, x\dot{v}_{p2} - y\dot{v}_{p1}). \quad (22)$$

Substituting Eqs. (17)-(22) into Eq. (15) gives

$$J_1(q\ddot{x} + s\ddot{y}) + n\dot{x} + y + v_{p2} = 0, \quad (23)$$

$$J_2(p\ddot{x} + q\ddot{y}) - n\dot{y} + x + v_{p1} = 0, \quad (24)$$

where

$$J_1 \equiv I_1 + 1 = \frac{b^2 + 6}{5}, \quad J_2 \equiv I_2 + 1 = \frac{a^2 + 6}{5}. \quad (25)$$

For \dot{n} , the following equation is obtained

$$\begin{aligned} I_3\dot{n} + q(x\ddot{x} - y\ddot{y}) + sx\ddot{y} - p\ddot{x}y + n(x\dot{x} + y\dot{y}) \\ + (q(y^2 - x^2) + (p-s)xy) + xv_{p2} - yv_{p1} = 0. \end{aligned} \quad (26)$$

Let v_{p1}, v_{p2} be expressed with respect to x, y and n from Eq. (20). Using Eqs. (14) and (24) and adopting approximations $(1 - \frac{1}{J_2}) \sim 1$ and $\frac{v_{p1}}{\mu} \sim O(\frac{1}{\mu^2}) \sim 0$ from Eq. (20), v_{p1} is given by

$$\begin{aligned} v_{p1} &\simeq -\frac{1}{\mu}(p\ddot{x} + q\ddot{y} - n\dot{y}), \\ &= -\frac{1}{\mu} \left(\frac{1}{J_2}(n\dot{y} - x - v_{p1}) - n\dot{y} \right), \\ &\simeq \frac{1}{\mu}(n\dot{y} + \frac{x}{J_2}). \end{aligned} \quad (27)$$

Similarly, v_{p2} is given by

$$v_{p2} \simeq -\frac{1}{\mu}(n\dot{x} - \frac{y}{J_1}). \quad (28)$$

By substituting Eqs. (27) and (28) in Eqs. (23)-(26), and neglecting $O(\frac{2}{\mu})(< O(q))$ terms, such as $(J_1q - \frac{2}{\mu})\ddot{x} \sim$

$J_1 q \ddot{x}$, at the leading order, the following equations are obtained:

$$J_1(q\ddot{x} + s\ddot{y}) + n\dot{x} + y + \frac{\dot{y}}{J_1\mu} = 0, \quad (29)$$

$$J_2(p\ddot{x} + q\ddot{y}) - n\dot{y} + x + \frac{\dot{x}}{J_2\mu} = 0, \quad (30)$$

$$I_3\dot{n} + q(x\ddot{x} - y\ddot{y}) + sx\ddot{y} - p\ddot{x}y + n(x\dot{x} + y\dot{y}) + (q(y^2 - x^2) + (p - s)xy) + \frac{x\dot{y}}{\mu J_1} - \frac{y\dot{x}}{\mu J_2} = 0. \quad (31)$$

From the above expressions, it is observed that the main parts are oscillations of x and y , such as $\ddot{y} + \frac{1}{J_1 s}y = 0$ and $\ddot{x} + \frac{1}{J_2 p}x = 0$. Moffatt and Tokieda[5] suggested that the terms $J_1 q \ddot{x}$, $n\dot{x}$, $J_2 q \ddot{y}$ and $n\dot{y}$ are crucial in creating reverse oscillations. The effect of friction is included in the terms $\frac{\dot{y}}{J_1\mu}$ and $\frac{\dot{x}}{J_2\mu}$.

Furthermore, to eliminate terms depending on $q\ddot{x}$ and $q\ddot{y}$, the new variables X and Y are defined as follows:

$$\begin{pmatrix} X \\ Y \end{pmatrix} \equiv TJP \begin{pmatrix} x \\ y \end{pmatrix}, \quad (32)$$

where

$$J \equiv \begin{pmatrix} \sqrt{J_2} & 0 \\ 0 & \sqrt{J_1} \end{pmatrix}, P \equiv \begin{pmatrix} p & q \\ q & s \end{pmatrix}.$$

In Eq. (32), matrix T is a rotational matrix that diagonalizes the symmetric matrix $Q \equiv J^{-1}P^{-1}J^{-1}$, and it is defined by

$$T \equiv \begin{pmatrix} \cos \theta & \sin \theta \\ -\sin \theta & \cos \theta \end{pmatrix}.$$

The matrix Q is expressed as

$$Q = \frac{1}{\Delta} \begin{pmatrix} \frac{s}{J_2} & -\frac{q}{\sqrt{J_1 J_2}} \\ -\frac{q}{\sqrt{J_1 J_2}} & \frac{p}{J_1} \end{pmatrix}.$$

The rotational angle θ is given by

$$\begin{aligned} \tan 2\theta &= -\frac{2q\sqrt{J_1 J_2}}{J_1 s - J_2 p} \\ &\sim -\frac{2\sqrt{2}}{5}\delta ab \sim O(10^{-1}) \end{aligned} \quad (33)$$

The eigenvalues of Q , ν_1 and ν_2 , correspond to the frequencies of X and Y , respectively, and they are given as follows:

$$F \equiv TQT^{-1} = \begin{pmatrix} \nu_1^2 & 0 \\ 0 & \nu_2^2 \end{pmatrix}.$$

For $a > b$, by using Eqs. (1)-(3) for the parameters p , q and s , respectively, eigenvalues ν_1 and ν_2 are given as follows:

$$\nu_1^2 \sim 5 \left(\frac{a^2}{a^2 + 6} + \delta^2 \frac{a^2}{6(1 - \frac{a^2}{b^2})} \right), \quad (34)$$

$$\nu_2^2 \sim 5 \left(\frac{b^2}{b^2 + 6} - \delta^2 \frac{a^2}{6(1 - \frac{a^2}{b^2})} \right). \quad (35)$$

The equations of motion with respect to X and Y are given by

$$(D^2 + F + DRF) \begin{pmatrix} X \\ Y \end{pmatrix} = \begin{pmatrix} 0 \\ 0 \end{pmatrix}$$

where

$$R \equiv TJ^{-1}NJT^{-1},$$

$$N \equiv \begin{pmatrix} 0 & -n \\ n & 0 \end{pmatrix}, D \equiv \begin{pmatrix} \frac{d}{dt} & 0 \\ 0 & \frac{d}{dt} \end{pmatrix}.$$

The matrix R has components a_i as follows:

$$R = \begin{pmatrix} a_1 & a_2 \\ a_3 & a_4 \end{pmatrix}, \quad (36)$$

where a_i are defined by

$$\begin{aligned} a_1 &\equiv m_1 - nk_1, \quad a_2 \equiv -m_2 - nk_2, \\ a_3 &\equiv -m_3 + nk_3, \quad a_4 \equiv m_4 + nk_4. \end{aligned} \quad (37)$$

In these equations, k_i are given by

$$k_1 \equiv -\nu_1^2 \sin \theta \cos \theta (f - f^{-1}) \sim a^2 \delta \sim O(1), \quad (38)$$

$$k_2 \equiv \nu_2^2 (f \sin^2 \theta + f^{-1} \cos^2 \theta) \sim \frac{5b}{\sqrt{2}a} \sim O(1), \quad (39)$$

$$k_3 \equiv \nu_1^2 (f \cos^2 \theta + f^{-1} \sin^2 \theta) \sim \frac{5a}{\sqrt{2}b} \sim O(10), \quad (40)$$

$$k_4 \equiv -\nu_2^2 \sin \theta \cos \theta (f - f^{-1}) \sim \frac{\delta a^2}{2} \sim O(1), \quad (41)$$

and m_i depending on friction parameter μ are given as follows:

$$m_1 \equiv \frac{f}{J_2\mu} \frac{\nu_1^2}{\nu_2^2} k_2, \quad m_2 \equiv \frac{f}{J_2\mu} k_4, \quad (42)$$

$$m_3 \equiv \frac{f}{J_2\mu} k_1, \quad m_4 \equiv \frac{f}{J_2\mu} \frac{\nu_2^2}{\nu_1^2} k_3. \quad (43)$$

where f is defined by

$$f \equiv \sqrt{\frac{J_2}{J_1}} = \sqrt{\frac{a^2 + 6}{b^2 + 6}}. \quad (44)$$

Finally, the effective equations of motion are obtained as follows:

$$\ddot{X} + \nu_1^2 X + a_1 \dot{X} + a_2 \dot{Y} = 0, \quad (45)$$

$$\ddot{Y} + \nu_2^2 Y + a_3 \dot{X} + a_4 \dot{Y} = 0, \quad (46)$$

$$I_3 \dot{n} - (X, Y) (KD^2 - K - SD) \begin{pmatrix} X \\ Y \end{pmatrix} = 0. \quad (47)$$

Here, S and K are 2×2 matrices as follows:

$$K \equiv \begin{pmatrix} k_1 & -k_3 \\ k_2 & -k_4 \end{pmatrix}, \quad S \equiv \begin{pmatrix} s_1 & s_2 \\ s_3 & s_4 \end{pmatrix}, \quad (48)$$

where s_i are defined by

$$\begin{aligned} s_1 &\equiv \nu_1^2(n\sqrt{J_1 J_2}k_3 - \frac{k_1}{\mu}), \\ s_2 &\equiv \nu_2^2(n\sqrt{J_1 J_2}k_1 + \frac{k_3}{\mu}), \\ s_3 &\equiv \nu_1^2(n\sqrt{J_1 J_2}k_4 - \frac{k_2}{\mu}), \\ s_4 &\equiv \nu_2^2(n\sqrt{J_1 J_2}k_2 + \frac{k_4}{\mu}). \end{aligned}$$

From Eqs. (42) and (43), it is found that these m_i are approximated as $m_i \sim \frac{k_i}{a\mu}$. When $n \sim O(10^{-2})$ and $\frac{1}{\mu} \sim O(10^{-2})$ are considered, a_i take a value of the order $O(10^{-1})$; therefore, I will neglect the quantities of $O(a_i^2)$ in the next section. For the no-slip case - (μ is sufficiently large),

$$m_i \sim 0. \quad (49)$$

Thus, it is observed that the effect of friction is included as $\frac{1}{\mu}$ in the m_i parameters.

IV. SLOWLY VARYING MODE

The motion of a rattleback contains a rapid frequency rattling mode and a slowly varying amplitude mode. To discuss the number of spin reversals, the slowly varying mode should be analyzed. In this section, by approximately solving the characteristic equation and considering the time average of the rapid frequency mode, the equations of the slowly varying mode is derived from the effective equations of motion which were obtained in the previous section.

To study the mode contained in $X(t)$ and $Y(t)$, I approximately solve the characteristic equation given in Eqs. (45) and (46). In this case, n is considered to be a constant, because \dot{n} is a second-order term from Eq. (31). Moreover, the quantities of $O(a_i^2)$ are neglected as explained in the previous section.

Two modes are observed, which correspond to the rattling motion of the long axial direction $e^{i\nu_1 t}e^{-\frac{a_1}{2}t}$ and the short axial direction $e^{i\nu_2 t}e^{-\frac{a_4}{2}t}$. Then, the mode expansions of $X(t)$ and $Y(t)$ are given by

$$\begin{aligned} X(t) &= c_1 e^{i\lambda_1 t} + c_1^* e^{-i\lambda_1^* t} + c_2 e^{i\lambda_2 t} + c_2^* e^{-i\lambda_2^* t}, \\ Y(t) &= d_1 e^{i\lambda_1 t} + d_1^* e^{-i\lambda_1^* t} + d_2 e^{i\lambda_2 t} + d_2^* e^{-i\lambda_2^* t}, \end{aligned}$$

where $\lambda_1 \equiv \nu_1 + i\frac{a_1}{2}$, $\lambda_2 \equiv \nu_2 + i\frac{a_4}{2}$, and $*$ indicates a complex conjugate. The coefficients c_1 , c_2 , d_1 and d_2 are obtained from $X(t)$ satisfying the equation of motion (Eq. (45)) and initial conditions such as $X(0) = x_0$,

$Y(0) = y_0$, $\dot{X}(0) = 0$ and $\dot{Y}(0) = 0$ as follows:

$$\begin{aligned} c_1 &\sim \left(\frac{1}{2} - i\frac{a_1}{4\nu_1}\right)x_0 + i\frac{a_2\nu_2^2}{2\nu_1\Delta}y_0, \\ c_2 &\sim -i\frac{a_2\nu_2}{2\Delta}y_0, \\ d_1 &\sim -i\frac{a_1^2}{8a_2\nu_1}x_0, \\ d_2 &\sim -i\frac{a_1^2}{8a_2\nu_2}x_0 + \left(\frac{1}{2} - i\frac{a_4}{4\nu_2}\right)y_0, \end{aligned}$$

where $\Delta \equiv \nu_1^2 - \nu_2^2$.

To obtain the behavior of $n(t)$, I consider the time average of the terms in the rapidly varying mode such as $e^{i\nu_i t}$, which are contained in terms, such as X^2 and $X\dot{X}$, of the equation for $\dot{n}(t)$. When the variables are given by $Q_1(t) = F_1(t)S_1(t)$ and $Q_2(t) = F_2(t)S_2(t)$, (where $F_i(t)$ are rapidly varying functions and $S_i(t)$ are slowly varying functions such as $e^{-\frac{a_i}{2}t}$), the time average of Q_1 and Q_2 ($\langle Q_1 Q_2 \rangle$) is defined as follows:

$$\langle Q_1 Q_2 \rangle \equiv S_1 S_2 \lim_{T \rightarrow \infty} \frac{1}{T} \int_0^T F_1 F_2 dt.$$

Then, neglecting terms $O(a_i^2)$,

$$\begin{aligned} \langle X^2 \rangle &\sim \frac{x_0^2}{2}e^{-a_1 t}, \quad \langle X\dot{X} \rangle \sim -\frac{x_0^2}{4}a_1 e^{-a_1 t}, \\ \langle X\ddot{X} \rangle &\sim -\frac{\nu_1^2 x_0^2}{2}e^{-a_1 t}, \\ \langle X\dot{Y} \rangle &\sim \frac{a_1^2}{8a_2}x_0^2 e^{-a_1 t} - \frac{a_2\nu_2^2}{2\Delta}y_0^2 e^{-a_4 t} \sim -\langle Y\dot{X} \rangle, \\ \langle Y^2 \rangle &\sim \frac{y_0^2}{2}e^{-a_4 t}, \quad \langle Y\dot{Y} \rangle \sim -\frac{y_0^2}{4}a_4 e^{-a_4 t}, \\ \langle Y\ddot{Y} \rangle &\sim -\frac{\nu_2^2 y_0^2}{2}e^{-a_4 t}, \\ \langle XY \rangle &\sim 0, \quad \langle X\ddot{Y} \rangle \sim 0. \end{aligned}$$

From these equations, it is observed that $\langle X\dot{X} \rangle$ and $\langle Y\dot{Y} \rangle$ are $O(a_i)$. Thus, the main part of \dot{n} is obtained as follows:

$$\begin{aligned} I_3 \dot{n}(t) &\sim k_1(\langle X\ddot{X} \rangle - \langle X^2 \rangle) - k_4(\langle Y\ddot{Y} \rangle - \langle Y^2 \rangle) \\ &= -\frac{k_1}{2}A^2 + \frac{k_4}{2}B^2, \end{aligned} \quad (50)$$

where

$$A \equiv \sqrt{\nu_1^2 - 1}x_0 e^{-\frac{a_1}{2}t}, B \equiv \sqrt{\nu_2^2 - 1}y_0 e^{-\frac{a_4}{2}t}. \quad (51)$$

From the definitions given in Eq. (51), these variables satisfy the differential equations by using the approximation $\dot{n} \sim 0$ as follows:

$$\dot{A} = -\frac{a_1}{2}A, \quad \dot{B} = -\frac{a_4}{2}B. \quad (52)$$

In the no-slip case (μ is sufficiently large), from Eq. (49), the parameters a_1 and a_4 are given as $a_1 = -nk_1$ and

$a_4 = nk_4$, respectively. Then, substituting these parameters into Eqs. (50) and (52) gives equations that correspond to those obtained by Pascal[2], Markeev[3] and Moffatt and Tokieda[5].

Multiplying Eq. (50) by n and using Eqs. (37) and (52), the following equation is obtained:

$$\frac{d}{dt}(N^2 + A^2 + B^2) = -m_1 A^2 - m_4 B^2, \quad (53)$$

where $N \equiv \sqrt{I_3}n$. For no-slip case ($m_i = 0$), the variable $E_1 \equiv N^2 + A^2 + B^2$ corresponds to the sum of energy about the rotation N , and the amplitudes of the long and short axial directions (A and B , respectively) are conserved. Moreover, from Eq. (52), it is observed that the variable $E_2 \equiv A^\gamma B$ is conserved, where $\gamma \equiv \frac{k_4}{k_1}$. In the phase spaces of N , A and B , E_1 corresponds to a sphere and E_2 corresponds to a quasi-hyperbolic cylinder. The trajectories of the system are closed curves that intersect this cylindrical surface and the sphere. Therefore, an infinite number of spin reversals is obtained.

In contrast, for the slip case, it is observed that the energy E_1 decreases according to the right-hand-side of Eq. (53), which relates to friction. By using the approximation $\dot{n} \sim 0$, it is assumed that γ is almost constant and E_2 is almost conserved; then, the trajectory of the system decreases as the radius of the sphere of E_1 decreases. Therefore, a finite number of spin reversals is obtained.

V. NEW PHENOMENON FOR THE SLIP CASE

For the no-slip case, rattle vibration increases irrespective of how small the initial spin n_0 is, and in theory, spin reversal occurs. However, for the slip case, when n_0 is small, vibration does not increase, and rotation stops. Even if rattle vibration occurs, spin reversal does not. Thus, a critical value of the spin n_{c1} may exist under which rattle vibration does not increase, and a critical value of the spin n_{c2} may exist under which rattle vibration increases but spin reversal does not occur. Therefore, it is assumed that the number of spin reversals is finite due to the existence of these critical spin values. In this section, I discuss some facts relating to these values.

A. Critical spin n_{c1} necessary to increase rattle vibration

For spin reversal to occur, rattle vibration must increase. This vibration increases according to the factor $e^{-a_1 t}$ and $e^{-a_4 t}$. For the no-slip case, these factors are $e^{+nk_1 t}$ and $e^{-nk_4 t}$. From Eqs. (38) and (41), it is observed that nk_1 and nk_4 have the same sign and if one mode increases, the other decreases. In contrast, for the slip case, m_1 and m_4 are in a_1 and a_4 ; hence, $a_1 > 0$ and $a_4 > 0$ occur according to the value of n . In this

case, both modes decrease, and rattle vibration does not increase. The spin values $n_{c1\pm}$ are given by

$$n_{c1+} \equiv \frac{m_1}{k_1} = -\frac{\cos^2 \theta + f^2 \sin^2 \theta}{J_2 \mu \sin \theta \cos \theta (f - f^{-1})},$$

$$n_{c1-} \equiv -\frac{m_4}{k_4} = \frac{f^2 \cos^2 \theta + \sin^2 \theta}{J_2 \mu \sin \theta \cos \theta (f - f^{-1})},$$

for $k_1 > 0$. For the case of $k_1 < 0$, these values reverse and are given by $n_{c1+} = -\frac{m_4}{k_4}$ and $n_{c1-} = \frac{m_1}{k_1}$. Therefore, it is observed that rattle vibration decreases for the initial spin n_0 in the range $n_{c1-} < n_0 < n_{c1+}$.

B. Critical spin n_{c2} necessary to reverse rattleback spin

When the spin is more than n_{c1} , rattle vibration increases. However, the spin does not necessarily reverse. A critical spin value n_{c2} may exist over which spin reversal occurs.

When starting with $n_0 > 0$, although it is near the value of n_0 , for a while, rattle vibration begins rapidly, and spin decreases. Eventually, the rattleback stops spinning and then reverses direction, and the spin value decreases to $n_1 < 0$. This spin value n_1 is obtained as follows.

Now, consider the case for $k_1 > 0$, $k_4 > 0$ and $n_0 > 0$. At first, the modes A and B exponentially increase and decrease, respectively: therefore, from Eq. (50), \dot{n} approximates to

$$I_3 \dot{n} \simeq -\frac{k_1 \nu_1^2}{2} A^2. \quad (54)$$

Integrating this equation from $t_0 (n = n_0 > 0)$ to $t_1 (n = n_1)$ gives

$$I_3 (n_1 - n_0) = -\frac{k_1 \nu_1^2}{2} \int_{t_0}^{t_1} A^2. \quad (55)$$

Furthermore, Eq. (53) approximates to

$$\frac{d}{dt}(I_3 n^2 + \nu_1^2 A^2) \simeq -m_1 \nu_1^2 A^2. \quad (56)$$

Integrating this equation gives

$$\nu_1^2 \int_{t_0}^{t_1} A^2 \simeq -\frac{I_3}{m_1} (n_1^2 - n_0^2), \quad (57)$$

where it is considered that $A(t_0) \sim 0$ and $A(t_1) \sim 0$. By substituting Eq. (57) into Eq. (55), n_1 is given by

$$n_1 = -n_0 + \frac{2m_1}{k_1}. \quad (58)$$

Then it is observed that if $n_1 < 0$, that is, the initial spin $n_0 > \frac{2m_1}{k_1}$, one spin reversal occurs, and if $n_0 \leq \frac{2m_1}{k_1}$, no spin reversal occurs. Therefore, it is observed that if $n_{c1+} = \frac{m_1}{k_1} < n_0 \leq \frac{2m_1}{k_1}$, rattle vibration increases but spin reversal does not occur. Similarly, when $n_0 < 0$, the

condition $n_0 < -\frac{2m_4}{k_4}$ must be satisfied for spin reversal to occur.

Finally, it is observed that there exist critical spins $n_{c2\pm}$ as follows:

$$n_{c2+} \equiv \frac{2m_1}{k_1}, \quad n_{c2-} \equiv -\frac{2m_4}{k_4}.$$

When $n_{c2-} \leq n_0 < n_{c1-}$ or $n_{c1+} < n_0 \leq n_{c2+}$, rattle vibration increases but spin reversal does not occur. For the case of $k_1 < 0$, it is observed that n_{c2-} and n_{c2+} are switched: $n_{c2-} = \frac{2m_1}{k_1}$ and $n_{c2+} = -\frac{2m_4}{k_4}$.

C. Number of spin reversals n_r

For the no-slip case, because dynamical energy is conserved, an infinite number of spin reversals occur. In contrast, for the slip case, because friction exist, the number of spin reversals n_r is finite.

As discussed in the previous section, for $n_1 < 0$, the condition for the first spin reversal occurrence is given by

$$\frac{1}{h_1} > 1, \quad (59)$$

where

$$h_1 \equiv \left| \frac{2m_1}{k_1 n_0} \right|. \quad (60)$$

Next, for the second spin reversal, if n_1 satisfy $n_1 > n_{c1-} = -\frac{m_4}{k_4}$, rattle vibration does not increase and the rattleback stops spinning. If n_1 satisfy $n_{c1-} > n_1 > n_{c2-} = -\frac{2m_4}{k_4}$, rattle vibration increases but spin reversal does not occur. Therefore, the condition for the second spin reversal to occur is as follows:

$$n_1 < -\frac{2m_4}{k_4}. \quad (61)$$

Now, I shall estimate spin n_2 after the second rattle vibration. Similar to the derivation of n_2 in the previous section, the following equation is obtained:

$$\begin{aligned} n_2 &= -n_1 - \frac{2m_4}{k_4} \\ &= n_0 - \frac{2m_1}{k_1} - \frac{2m_4}{k_4}. \end{aligned}$$

Thus, if $n_2 > 0$, the second spin reversal occurs. This condition is consistent with Eq. (61). The condition for the second spin reversal occurrence is given by

$$\frac{1}{h_1} > 1 + \rho, \quad (62)$$

where

$$\rho \equiv \frac{h_4}{h_1}, \quad h_4 \equiv \left| \frac{2m_4}{k_4 n_0} \right|.$$

From Eqs. (59) and (62), the condition that spin reversal occurs only once is given by $1 < \frac{1}{h_1} \leq 1 + \rho$. Similarly,

the condition that spin reversal occurs only two times is given by $1 + \rho < \frac{1}{h_1} \leq 2 + \rho$, only three is given by $2 + \rho < \frac{1}{h_1} \leq 2 + 2\rho$, and so on.

It is observed that the number of spin reversals n_r satisfies the following inequalities:

$$\text{iIj} n_0 > 0, k_1 > 0, k_4 > 0 \text{ or } n_0 < 0, k_1 < 0, k_4 < 0$$

$$K_0(n_r - 1, \rho) < \frac{1}{h_1} \leq K_0(n_r, \rho), \quad (63)$$

$$\text{iiIj} n_0 > 0, k_1 < 0, k_4 < 0 \text{ or } n_0 < 0, k_1 > 0, k_4 > 0$$

$$K_1(n_r - 1, \rho) < \frac{1}{h_1} \leq K_1(n_r, \rho), \quad (64)$$

where

$$K_0(n, \rho) \equiv \sum_{i=0}^n P_+(i) + P_-(i)\rho,$$

$$K_1(n, \rho) \equiv \sum_{i=0}^n P_+(i)\rho + P_-(i),$$

$$P_{\pm}(i) \equiv \frac{1 \pm (-1)^i}{2}.$$

Finally, from the inequalities stated in Eqs. (63) and (64), the number of spin reversals n_r are obtained.

For case (I), n_r is given by

$$n_r = \begin{cases} 2[x] + 1 & \text{if } x - 1 \leq [x] < x - \frac{1}{1+\rho} \\ 2[x] & \text{if } x - \frac{1}{1+\rho} \leq [x] < x \end{cases} \quad (65)$$

and for case (II), n_r is given by

$$n_r = \begin{cases} 2[x] + 1 & \text{if } x - 1 \leq [x] < x - 1 + \frac{1}{1+\rho} \\ 2[x] & \text{if } x - 1 + \frac{1}{1+\rho} \leq [x] < x \end{cases} \quad (66)$$

where x is defined by

$$x \equiv \frac{1}{h_1(\rho + 1)},$$

and $[x]$ is Gauss' symbol, which represents the greatest integer less than or equal to x .

D. Relationship between number of spin reversals and rattleback shape

In this subsection, the relationship among the number of spin reversals, the axis inclination ($\delta \sim \theta$ in Eq. (33)), the coefficient of friction μ and the rattleback shape are obtained.

The factor $x = \frac{1}{h_1(\rho+1)}$ is written as

$$x = \frac{1}{2} J_2 \mu |n_0 \sin \theta \cos \theta| L(f),$$

where $L(f)$ is the form factor given by

$$L(f) \equiv \frac{|f - f^{-1}|}{1 + f^2}. \quad (67)$$

This expression shows that the number of spin reversals is proportional to the coefficient of friction μ , the axis inclination δ , and the initial spin n_0 . Therefore, when the friction is large (close to the no-slip case) and the asymmetry between the shape axes and the principal inertia axes is large, the number of spin reversal becomes large.

Here, I discuss the form factor $L(f)$. When the long axis a is fixed, which responds to a fixed J_2 , enlarging f correspond to reduction in J_1 from Eq. (44). Furthermore, from Eq. (25), reducing J_1 corresponds to a reduction in b , which indicates that the rattleback becomes long and slender. In contrast, reducing f results in the rattleback becoming more circular, such as $J_1 = J_2$. The form factor $L(f)$ has maximum at $f = \sqrt{2 + \sqrt{5}}$. Thus, it is observed that if the rattleback long and slender, rattle vibration about the short axis does not easily occur and the number of spin reversals is reduced. This also occurs, if the rattleback is more circular. The relationship between a and b corresponding to the maximum of f is given by

$$b^2 = \frac{a^2 + 6}{2 + \sqrt{5}} - 6. \quad (68)$$

For example, if $a = 10$, b becomes approximately 4.4. Fig. 3 shows the change in the form factor $L(f)$ when $a = 10$ is fixed and b is varied from 1 to 10. It is observed that there is a maximum value around $b \sim 4.4$.

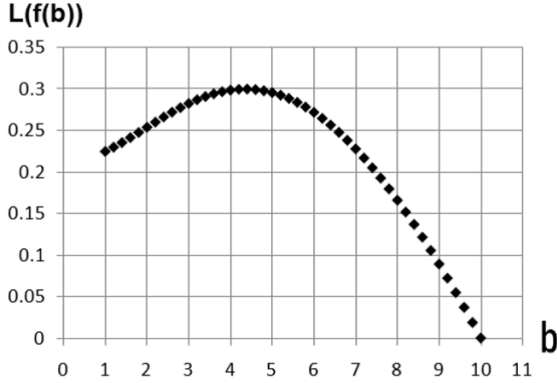


FIG. 3. Form factor $L(f)$ versus b for $a = 10$

VI. NUMERICAL RESULTS

④In this section, the results of computations based on the exact system described in Eqs. (6)-(10) are presented and these results are compared with those based on the effective equations of motion described in Eqs. (45)-(47).

For the numerical simulations, the NDSolve command in *Mathematica* is used.

A. Validity of the approximation $\dot{v}_0 \gg \dot{v}_p$

In section III, the approximation $\dot{v}_0 \gg \dot{v}_p$ was used to derive effective equations of motion.

The initial conditions are $x_0 = y_0 = 0.01$, $\dot{x}_0 = \dot{y}_0 = 0$ and $n_0 = 0.05$ with parameters $a = 10$, $b = 3$, and $\delta = 0.03$. Fig. 4 shows the behavior of \dot{v}_{01} and \dot{v}_{p1} for $\mu = 100$, and Fig. 5 shows the behavior of \dot{v}_{02} and \dot{v}_{p2} for $\mu = 100$. From Figs. 4 and 5, the comparison of the

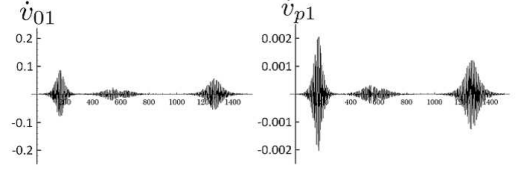


FIG. 4. Time evolution of \dot{v}_{01} and \dot{v}_{p1} for $\mu = 100$

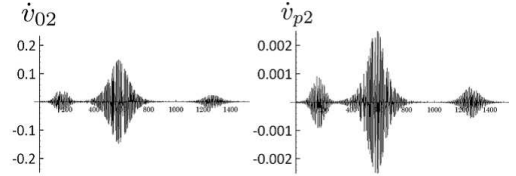


FIG. 5. Time evolution of \dot{v}_{02} and \dot{v}_{p2} for $\mu = 100$

amplitudes shows that $\dot{v}_{p1} \sim \dot{v}_{01} \times \frac{1}{50}$ and $\dot{v}_{p2} \sim \dot{v}_{02} \times \frac{1}{50}$; therefore, it can be safely assumed that $\dot{v}_{01} \gg \dot{v}_{p1}$ and $\dot{v}_{02} \gg \dot{v}_{p2}$. Figs. 6 and 7 are the same as Figs. 4 and 5, respectively, but for $\mu = 200$. In this case, it is similarly

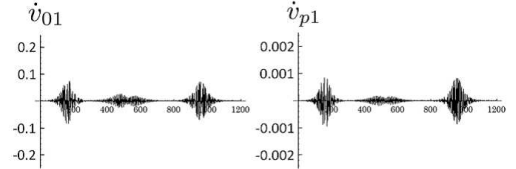


FIG. 6. Time evolution of \dot{v}_{01} and \dot{v}_{p1} for $\mu = 200$

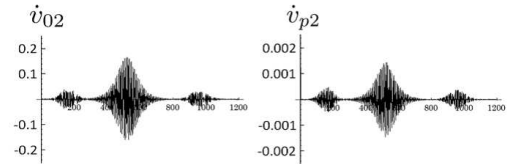


FIG. 7. Time evolution of \dot{v}_{02} and \dot{v}_{p2} for $\mu = 200$

shown that $\dot{v}_{p1} \sim \dot{v}_{01} \times \frac{1}{100}$ and $\dot{v}_{p2} \sim \dot{v}_{02} \times \frac{1}{100}$; therefore, $\dot{v}_{01} \gg \dot{v}_{p1}$ and $\dot{v}_{02} \gg \dot{v}_{p2}$. Note that the approximation improves when μ increases. Thus, it can be concluded that the approximation $\dot{v}_0 \gg \dot{v}_p$ is valid.

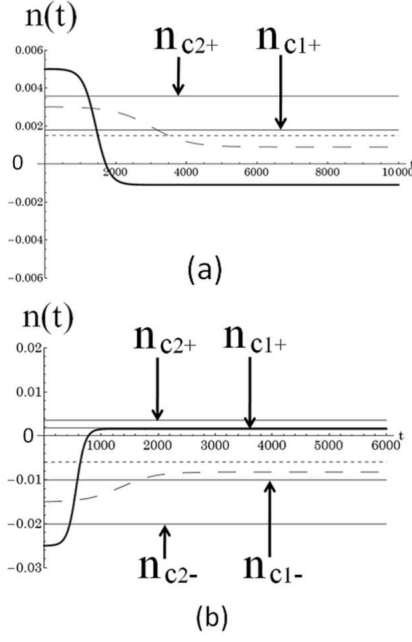


FIG. 8. Time evolution of $n(t)$ with (a) positive initial spin with $n_0 = 0.0015$ (dotted line), 0.003 (dashed line), and 0.005 (solid line) and (b) negative initial spin with $n_0 = -0.006$ (dotted line), -0.015 (dashed line) and -0.025 (solid line).

B. $n_{c1\pm}$, $n_{c2\pm}$, and spin reversal behavior

In subsections VA and VB of section V, the critical values of spin necessary to increase rattle vibration and cause spin reversal are obtained. Here, computational results for these values and the spin reversal behavior which are obtained from a simulation based on the exact system are presented.

The initial conditions are $x_0 = y_0 = 0.01$, and $\dot{x}_0 = \dot{y}_0 = 0$ with parameters $a = 10$, $b = 3$, and $\delta = 0.03$. The coefficient of friction is set to $\mu = 75$. For these initial conditions, the following critical spin are obtained: $n_{c2+} = 0.00358$, $n_{c1+} = 0.00179$, $n_{c1-} = -0.01$, and $n_{c2-} = -0.0201$. Fig. 8 shows the computed evolution of $n(t)$. In Fig. 8 (a), as discussed in subsection VA, the dotted line with the initial spin $n_0 = 0.0015 < n_{c1+}$ shows that rattle vibration does not increase. As discussed in subsection VB, the dashed line with the initial spin $n_{c1+} < n_0 = 0.003 < n_{c2+}$ shows that rattle vibration increases but spin reversal does not occur. The solid line with the initial spin $n_{c2+} < n_0 = 0.005$ shows that the spin reversal behavior agrees with that discussed in subsection VB. Fig. 8 (b) shows the behavior of $n(t)$ for negative initial spins $n_0 = -0.006$ (dotted line), -0.015 (dashed line), and -0.025 (solid line). Even if the initial spin is negative, the same behavior occurs about n_{c1-} and n_{c2-} . Thus, it is observed that spin reversal behaviors are depended on these critical values.

C. Number of spin reversals n_r and friction coefficient μ

This subsection discusses how the number of spin reversals n_r changes depending on the friction coefficient μ . This number of spin reversals is obtained from a simulation based on the exact system described in Eqs. (6)-(10).

The initial conditions are $x_0 = y_0 = 0.01$, $\dot{x}_0 = \dot{y}_0 = 0$, and $n_0 = 0.05$ with parameters $a = 10$, $b = 3$, and $\delta = 0.03$. Fig. 9 (a) shows the behavior of $n(t)$ for $\mu = 60$ (solid line), 130 (dotted line) and 200 (dashed line). It is observed that for each of these μ values, the number of spin reversals increases to three, six, and nine times, respectively. Fig. 9 (b) shows the behavior of spin $n(t)$ for $\mu = 500$ (solid line), 1000 (dotted line), 1500 (dashed line). Note that the spin behavior is similar to that for the no-slip case as the friction increases.

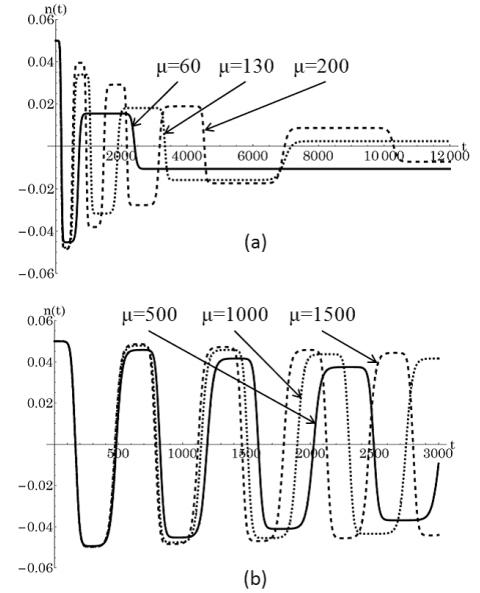


FIG. 9. Time evolution of $n(t)$. (a) The initial values of μ are 60 (solid line), 130 (dotted line), and 200 (dashed line). (b) The initial values of μ are 500 (solid line), 1000 (dotted line), and 1500 (dashed line).

We usually consider that when friction enlarge, energy loss become large, so that the reverse number decrease. The numerical simulations show the opposite thing to this intuition. In reality, the contact with the horizontal plane is not a point but an area, spinning torque by rotation n seems to effect the dynamics of rattleback as discussed by Garcia and Hubbard[9]. The adopted model does not include this spinning torque, so that energy loss depends only on the velocity \mathbf{v}_p which becomes small when friction coefficient μ becomes large, thus, it may be considered that the number of spin reversal increase. Moreover, in reality, when the spin reversal does not occur, the contact point x_p settles down to $x = y = 0$ and $z = 1$, and the slip velocity \mathbf{v}_p is equal to zero. Then,

the rattleback stops spinning after a while. In contrast, in the numerical simulation, if we set the conditions $\mathbf{v}_p = 0$, $\ddot{x} = \dot{x} = x = 0$, and $\ddot{y} = \dot{y} = y = 0$, \dot{n} becomes zero from Eq. (26). Therefore, the spin $n(t)$ becomes constant and does not stop after the spin reversal ends, as shown in Fig. 9 (a). It is considered that this phenomena are also depended on not considering spinning torque due to the frictional force by spinning.

D. The approximate number of spin reversals $n_{r:ap}$ versus the exact number of spin reversals $n_{r:ex}$

In this subsection, the approximate number of spin reversals $n_{r:ap}$ obtained from Eqs. (65) and (66) in subsection V C is compared with the exact number of spin reversals $n_{r:ex}$ obtained from a simulation based on the exact system described in Eqs. (6)-(10).

The initial conditions are $x_0 = y_0 = 0.01$, $\dot{x}_0 = \dot{y}_0 = 0$ and $n_0 = 0.05$ with parameters $a = 10$, $b = 3$, and $\delta = 0.03$. Fig. 10 shows the number of spin reversals n_r for a range of values of μ from 20 to 200. Crosses represent $n_{r:ex}$ and the boxes represent $n_{r:ap}$. Up to $\mu \sim 70$, both

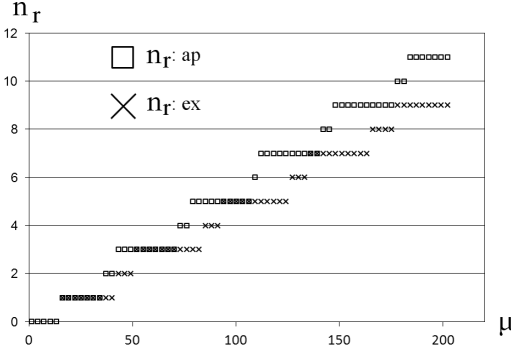


FIG. 10. The number of spin reversals n_r versus μ : \square represents $n_{r:ap}$ and \times represents $n_{r:ex}$

values are almost identical, but, the difference increases as μ increases. It is assumed that the terms neglected in the approximation affect energy dissipation. Thus, for a given value of μ , $n_{r:ap}$ is larger than $n_{r:ex}$.

E. Form factor $L(f)$ and $n_{r:ex}$

This subsection discusses the relationship between the form factor defined in Eq. (67) and $n_{r:ex}$.

The initial conditions are $x_0 = y_0 = 0.01$, $\dot{x}_0 = \dot{y}_0 = 0$, and $n_0 = 0.05$ with parameters $a = 10$, and $\delta = 0.03$. Fig. 11 shows the behavior of $n_{r:ex}$ as a function of the parameter b for $\mu = 100$ and 200. Note that the b dependence of $n_{r:ex}$ is similar to that of the form factor presented in Fig. 3. Therefore, the estimate derived from

the effective equations of motion is qualitatively correct.

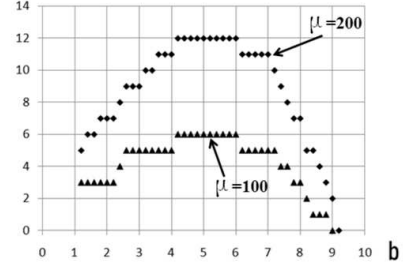


FIG. 11. Number of spin reversals $n_{r:ex}$ versus b

VII. DISCUSSION AND CONCLUSIONS

I have examined the behavior of a rattleback with viscous friction to answer the questions mentioned in the introduction. The following results were determined analytically and confirmed numerically.

Critical value of the initial spin exist: $n_{c1\pm}$ and $n_{c2\pm}$. When the initial spin n_0 is in the region $n_{c1-} < n_0 < n_{c1+}$, rattle vibration does not increase. When the initial spin n_0 is in the region $n_{c2-} < n_0 < n_{c1-}$ or $n_{c1+} < n_0 < n_{c2+}$, rattle vibration increases but spin reversal does not occur. A numerical simulation based on the exact equations of motion confirmed the existence of these values.

I theoretically obtained the number of spin reversals n_r as a function of the coefficient of friction μ and the form factor $L(f)$, which contains the ratio of a to b . From the expression of n_r , it was found that the number of spin reversals increases as μ increases and a certain value of the ratio of a to b gives the maximum number of spin reversals.

In this paper, viscous friction is adopted to perform a first examination of spin reversal. However, in reality it is assumed that spin reversal is associated with the effect of Coulomb friction. Furthermore, it seems that rolling friction and friction by spinning are also effective. Therefore, these frictions should be adopted to further understand the rattleback behavior. This is a subject for future investigations.

ACKNOWLEDGMENTS

I thank members of the elementary particle physics groups at Niigata University and Yamagata University for their valuable comments on my study in an autumn seminar at Bandai Fukushima in Japan(2010). I also appreciate the support received at a workshop hosted by the Yukawa Institute for Theoretical Physics at Kyoto University.

-
- [1] G.T.Walker, Quarterly journal of pure and applied mathematics **28**, 175 (1896)
 - [2] M.Pascal, Journal of Applied Mathematics and Mechanics **47**, 269 (1983)
 - [3] A.P.Markeev, Journal of Applied Mathematics and Mechanics **47**, 473 (1984)
 - [4] R. A.D.Blackowiak and H.Kaplan, in *Proceedings of DETC'97, ASME Design Engineering Technical Conferences* (1997)
 - [5] H.K.Moffatt and T.Tokieda, Proc. R. Soc. Edinburgh. A **138**, 361 (2008)
 - [6] H.Bondi, Proc. R. Soc. Lond. A **405**, 265 (1986)
 - [7] T.R.Kane and D.A.Levinson, I.J.Non-Linear Mechanics **17**, 175 (1982)
 - [8] R.E.Lindberg and R.W.Longman, Acta Mechanica **49**, 81 (1983)
 - [9] A.Garcia and M.Hubbard, Proc.R.Soc. Lond. A **148**, 165 (1998)
 - [10] A.V.Karapetian, Prikl.Matem.Mekhan **45**, 42 (1981)